STRUCTURE OF INCLUSIVE SPECTRA AND FLUCTUATIONS IN INELASTIC PROCESSES CAUSED BY MULTIPLE-POMERON EXCHANGE

V. A. Abramovskii and O. V. Kancheli
Institute of Physics of the Georgian Academy of Sciences

and

V. N. Gribov
Leningrad Institute for Nuclear Research

Introduction

Description of the asymptotics of strong interactions by means of the Pomeranchuk singularity (Pomeron-P) involves ideas both on processes of a diffractive type and inelastic processes giving the main contribution to total cross sections. As is well known starting with the work of Amati, Stanghellini, and Fubini[1] Pomeron-exchange, with the use of Feynman diagrams, may be described by a set of ladder-type diagrams

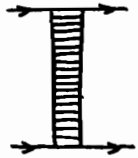

(1)

A characteristic feature of inelastic processes at asymptotic energies, described by the above diagrams, is a uniform distribution of produced particles (in the sense of inclusive cross sections) in rapidity (except the region of longitudinal momenta close to the momenta of colliding particles) that leads to the logarithmic increase in the multiplicity of produced particles, $\bar{n} \approx a\xi$, where $\xi = \ln(s/m_a m_b)$.

The second important feature of such diagrams is that in each individual event the uniform density appears only after averaging in fact a non-uniform distribution over ranges of rapidity larger than the characteristic scale $\lambda_0 \sim a^{-1} \sim 1$, determined by a ladder step. The probability of fluctuations with the scale much larger than λ_0 decreases exponentially.

It was understood that these properties do not require a description of the interaction literally by means of ladder diagrams, but may be caused by a more general phenomenon, by the absence of large transferred momenta at all stages of interaction.

As is well known, in addition to Pomeron exchange, the processes of exchange of several Pomerons, corresponding to branch points in the plane of complex angular momentum, give a considerable contribution to the interaction at high energy.

It is very interesting to determine what changes of the properties of inelastic processes are caused by taking into account multiple-Pomeron exchange. In this paper we shall try to analyze this problem. The Reggeon-diagram technique[2] was used to describe multiple-Pomeron exchange. The contribution to the total cross section of interaction corresponding to Pomeron exchange may be given by a number of diagrams of the form

$\sigma_{tot} =$ 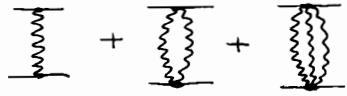 (2)

We shall show that even when multiple-Pomeron exchange and interactions of Pomerons are taken into account, we may preserve the first of the described properties of inelastic processes, i.e., the spectrum homogeneity (in the sense of inclusive cross sections) and $\bar{n} \sim \xi$. However, the scale of averaging at which the uniform density is reached and the probability of fluctuations (in each individual event) are found to be quite different. This difference from the ladder situation at $\xi \to \infty$ is caused only by Pomeron interactions. A uniform density appears only after averaging over a rapidity range $\geq \gamma\sqrt{\xi}$ where γ is determined by the triple-Pomeron vertex. The probability of fluctuations with the dimensions (in the space of rapidity) $\lambda > \gamma\sqrt{\xi}$ decreases as $\gamma^2\xi/\lambda^2$.

The distribution of large fluctuations is characterized by the following simple property: fluctuations of the dimensions λ are, on the average, at a distance of $\sim\lambda^2/\gamma^2 >> \lambda$, from one another in rapidity. It is interesting to note that for these large fluctuations the density of particles is either zero or double the mean density and the latter is encountered twice as often as the former.

On the whole the situation reminds one of the behavior of matter at the point of a second-order phase transition, when there are large fluctuations of the system in which various volumes of the matter are in different phase states.

The main content of the work is summarized in the following paragraphs. Our analysis proceeds from the representation of the total cross section as the sum of contributions of Reggeon diagrams and assuming that Reggeon exchange corresponds to a uniform density in rapidity (in the sense of the inclusive cross section) with the mean number of particles $\bar{n} \simeq a\xi$.

If Pomeron interactions are not taken into account the contribution of multiple-Pomeron exchange leads to the following phenomena. Corrections of the order $1/\xi$, $1/\xi^2$, . . . for partial cross sections σ_n appear in the main region $n \sim a\xi$. New processes are generated with the numbers of produced particles multiples of $\bar{n}$. Then the distribution over the number of particles has the form[3]

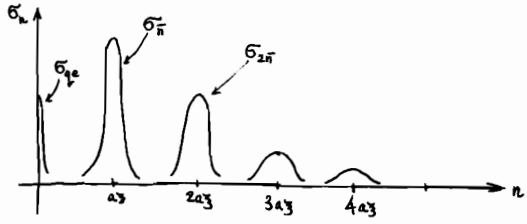

(3)

where the cross section $\sigma_{k\bar{n}} \sim 1/\xi^{k-1}$. Note that from the point of view of similarity with the gas models[4,5] the appearance of oscillations is associated with the finite dimensions of the system (the boundary effect). It turns out that corrections to the partial cross sections $\sigma_{\bar{n}}$ and the values of these cross sections $\sigma_{k\bar{n}}$, $k \neq 1$, are related in such a way that they cancel each other when the inclusive cross section is calculated. Let us explain by taking the example of two Pomeron exchange. Such an exchange leads to generation of new processes with the cross sections σ_{qe}, $\sigma_{2\bar{n}}$ and to a negative correction $\sigma'_{\bar{n}}$ caused by screening

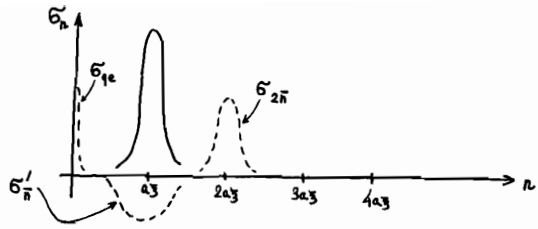

(4)

where $4\sigma_{qe} = -\sigma'_{\bar{n}} = 2\sigma_{2\bar{n}}$. Then the correction for the inclusive cross section in the central region is

$$\delta\left(\frac{\partial^3\sigma}{\partial p^3}\right) \sim \frac{\partial^3\sigma'_{\bar{n}}}{\partial p^3} + 2\frac{\partial^3\sigma_{2\bar{n}}}{\partial p^3} = 0. \tag{5}$$

Thus when Reggeon interactions are not taken into account the invariant inclusive cross section

$$f_1(\eta,\xi,p_\perp) = (2\pi)^3 2p_0 \frac{\partial^3\sigma}{\partial p^3} \tag{6}$$

(where $\eta \simeq \ln p_0$ is the rapidity of the observed particle in the central region) does not depend on η and ξ, up to corrections of order $1/s$.

When Reggeon interactions are taken into account, smoothing of the distribution σ_n takes place

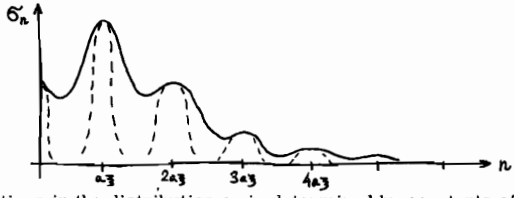

(7)

The amplitude of oscillations in the distribution σ_n is determined by constants of the Reggeon interactions.[3] The inclusive cross section of the process $p_a + p_b \to p + \{X\}$ in the central region contains logarithmic corrections in energy

$$f_i = \sigma_{tot}\,\psi(p_\perp^2)\left[1 + \frac{c_1}{\eta_1} + \frac{c_2}{\eta_2}\right], \tag{8}$$

where $\eta_1 = \ln(p_a + p)^2$, $\eta_2 = \ln(p_b + p)^2$ and the constants c_i are related to the value of the triple-Pomeron vertex. If all total cross sections are equal asymptotically[6] then f_1 will be universal within the accuracy $1/\eta_i$ and at the same time $c_1 = c_2$.

The correlation function of two particles produced in the central region with the rapidities η_1 and η_2 has the form

$$\rho_2(\eta_1,p_{1\perp};\eta_2,p_{2\perp}) \sim \psi(p_{1\perp}^2)\,\frac{3\gamma^2}{|\eta_1 - \eta_2|}\,\psi(p_{2\perp}^2). \tag{9}$$

The last section is devoted to studies of fluctuations in individual events. In particular, it is shown that the distribution over the number of fluctuations, the dimensions of which are

larger than λ where $\lambda >> \lambda_0$, is a Poisson distribution with the mean number of fluctuations

$$\overline{m(\lambda)} \sim \xi \gamma^2 / \lambda^2. \tag{10}$$

1. Absorptive Parts of Reggeon Diagrams in the s-Channel Classification of Inelastic Processes

Let us discuss first the structure of absorptive parts corresponding to the vacuum pole. It is known that the vacuum pole leads to a uniform spectrum of secondary particles of the type $\psi(p_\perp^2) d^3p/p_0$, where the function $\psi(p_\perp^2)$ should be assumed to decrease rapidly in $p_\perp^2$ for the self consistency of the whole scheme. Hence, the absorptive part of the pole may be shown as a generalized ladder, as indicated below, without specifying the character of the exchange in amplitudes $A_{2\to n}$.

$$(\text{abs})_s \left[A^{(\text{pol})}(s,t) \right] = (\text{abs})_s$$

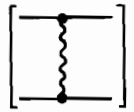

$$=$$

(11)

$$= \sum_n \int d\tau_n \left| A_{2\to n} \right|^2 = \sum_n \int d\tau_n$$

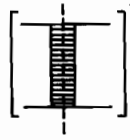

The simplest example of such amplitudes are multiperipheral ones,[7] but in general the real amplitudes $A_{2\to n}$ may be determined by many-particle exchange as well. The important thing is that states with large 4-momenta squared must be suppressed on virtual lines. In such a case intermediate states produced by the operation $(\text{abs})_s A^{(\text{pol})}$ will be approximately ordered by longitudinal momenta; only this fact reflects the chosen image of $A_{2\to n}$ in the form of a multiperipheral chain.

Having taken this picture of absorptive parts for the pole, let us consider what absorptive parts of two Reggeon cuts will not be small when $s \to \infty$. The simplest diagram with nonvanishing third spectral functions has the form

$A^{(2)} =$

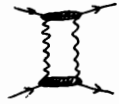

$\simeq$

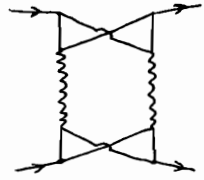

(12)

We see that when $(\text{abs})_s A^{(2)}$ is calculated, the dashed line corresponding to the diagram section may be drawn in different ways:

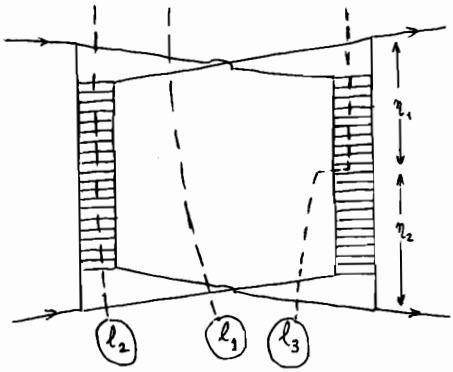

(13)

The different cuttings (for instance, ℓ_1, ℓ_2, ℓ_3 above) correspond, in fact, to nonequivalent inelastic processes, and for most of them [for instance, for ℓ_3 in (13)] the absorptive parts will not be expressed by quantities typical of Reggeon diagrams.

Let us determine what types of absorptive part are not small when $\xi = \ln s \to \infty$. We assert that the only cuttings of the diagram that are important are those in which the cutting line dividing the diagram into two parts does not leave the internal part of a Reggeon [as, for instance, the line ℓ_2 in (13)]. Qualitatively this may be explained in the following way. A cutting of the type ℓ_3, which violates the stated criterion, leads to the following diagram for many particle amplitudes

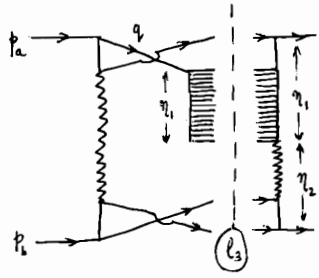

(14)

We see that in the "left-hand" amplitude $q^2 \sim M^2 e^{\eta_1} >> M^2$, because the internal part of a Reggeon has sense only when $\eta_1 >> 1$. Since we assume that large q^2 must be suppressed on <u>all</u> virtual lines, such absorptive parts will be asymptotically small. As for the region of small η_1, it contributes only to renormalization of the vertex entering the absorptive part.* It is easy to see that the described property of absorptive parts is common to all Reggeon diagrams. Cuts leaving the internal part of a Reggeon always lead to a "hanging multipheral chain" with a large mass and hence to large q_i^2 on the lines in the region of the peripheral chain attachment.

*Note that just the contributions of cuts with small η_1 are important in cancelling the main asymptotic terms in planar diagrams.[7]

Thus, the two-Reggeon diagram asymptotically has absorptive parts only of three types

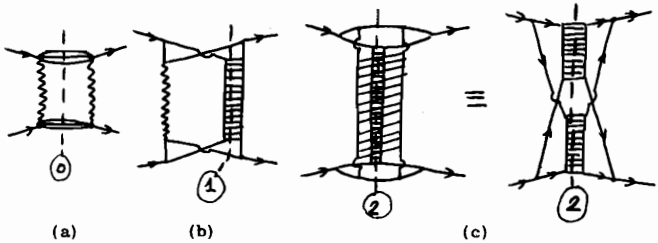

(a) (b) (c) (15)

determined by the number of cut Reggeons. Therefore, asymptotically the total absorptive part of the contribution of two Reggeon diagrams [$2\,\mathrm{Im}A^{(2)}$] is given by a sum of only three absorption parts corresponding to the cuts in (15).

$$2\,\mathrm{Im}A^{(2)} = F_0^{(2)} + F_1^{(2)} + F_2^{(2)}. \tag{16}$$

Similarly for the diagram

(17)

with ν Reggeons there will be $\nu+1$ types of absorptive parts not small asymptotically

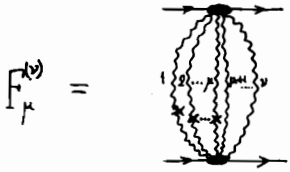

(18)

$$2\,\mathrm{Im}A^{(\nu)} = \sum_{\mu=0}^{\nu} F_\mu^{(\nu)}, \tag{19}$$

corresponding to simultaneous cutting of the μ ($\mu = 0, 1, 2, \ldots$) Reggeons marked with crosses.

This property of absorptive parts is easily generalized for diagrams with arbitrary Reggeon interactions. We see that for each Reggeon diagram for $A_{2\to 2}$ there are only several types of absorptive parts not small asymptotically. For instance, for the diagram

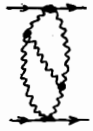

(20)

these parts will be

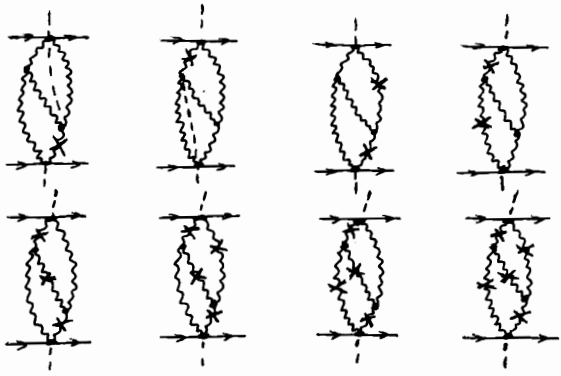

(20')

Let us now discuss what processes correspond to absorptive parts of Reggeon diagrams. In the simplest case of diagram (15a) the absorptive part corresponds to the process of production of a small number of particles with momenta close to those of incident particles, i.e., to quasi-elastic processes. The absorptive part of diagram (15b) corresponds to processes giving the main contributions to the cross section, to the same processes as the ones described by the absorptive part of the pole term with mean multiplicity equal to $a\xi$. Thus (15b) is a correction to the amplitudes of these main processes caused by screening. The absorptive part of diagram (15c) corresponds to processes with the mean density of particles per rapidity interval twice as large as that for processes corresponding to the pole term. These three absorptive parts lead to processes with the cross sections σ_{qe}, $\sigma'_{\bar{n}}$, $\sigma_{2\bar{n}}$ discussed in the introduction.

Similarly when cutting more complicated diagrams, absorptive parts appear corresponding either to corrections to the main processes, or processes in which at some rapidity interval there are no particles and in other intervals the particle density is a multiple of that in processes of the main type.

This result may be shown graphically in the following way. If we take an amplitude for the production of a given number of particles $n >> 1$ in the form of a combination of diagrams it is

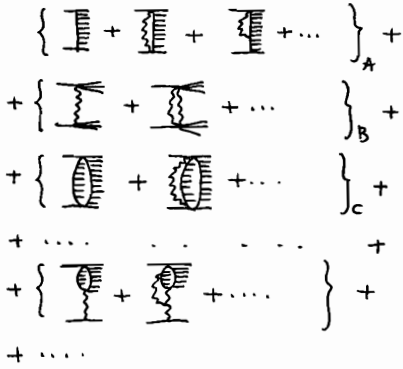

(21)

clear that, as functions of the kinematic variables of the particles, the amplitudes corresponding to diagrams of the classes A, B, ... do not overlap. Therefore, in calculation of the cross section, amplitudes corresponding to different classes do not interfere and the result may be shown symbolically in the form

$$\mathfrak{F}_A\mathfrak{F}_A^* + \mathfrak{F}_B\mathfrak{F}_B^* + \ldots \tag{22}$$

2. Relations Between Absorptive Parts of Reggeon Diagrams

It turns out that in a number of cases, the "not small" absorptive parts of a Reggeon diagram may be expressed in terms of the contribution of the Reggeon diagram itself, so that the only difference between them is some combinatory coefficient. (In particular, this holds for all absorptive parts of diagrams without interactions between Reggeons.) In other cases, new "cut" vertices of interactions between Reggeons will also enter the expression for the absorptive part.

Let us consider diagrams in (17). Their contributions to $A_{2\to 2}$ may be written in the form of an integral over two-dimensional transverse momenta of Reggeons

$$iA^{(\nu)}(s, Q^2) = s\int N_\nu [(i\mathfrak{D}_1)(i\mathfrak{D}_2)\ldots.(i\mathfrak{D}_\nu)] N_\nu d\Omega_\nu, \tag{23}$$

where

$$d\Omega_\nu = \frac{1}{\nu!}\,\delta^{(2)}\left(Q - \sum_1^\nu \kappa_i\right)\prod_1^\nu \frac{d^2\kappa_i}{2(2\pi)^2}$$

is the Reggeon phase space, $N_\nu(\vec{\kappa}_1, \ldots, \vec{\kappa}_\nu)$ are real vertices of Reggeon emission, $\mathfrak{D}(\xi, \vec{\kappa}^2)$ are complex Green functions of Reggeons. When a simple pole of positive signature corresponds to a Reggeon then

$$\mathfrak{D}(\xi, \kappa^2) = e^{-\alpha'\kappa^2\xi + \alpha(0) - 1}\,\frac{e^{-i\pi\alpha(\kappa^2)/2}}{\sin\frac{\pi\alpha(\kappa^2)}{2}} \tag{24}$$

The quantities in (24) N_ν, $d\Omega_\nu$ are real, and since we are going to be interested only in absorptive parts of $A^{(\nu)}$ in s, it is convenient to write expression (23) in a symbolic form

$$[-i(i\mathfrak{D}_1)(i\mathfrak{D}_2)\ldots.(i\mathfrak{D}_\nu)]. \tag{23'}$$

We omit the quantities N_ν here, since <u>they are not changed</u> by calculation of the absorptive parts of $A^{(\nu)}$ (see the Appendix).

Calculation of the absorptive parts of the amplitude $A^{(\nu)}$ is, in fact, of a combinatory character. Let us demonstrate the combinatorics, taking as an example the two-Reggeon cuts, where

$$A^{(2)} = [-i(i\mathfrak{D}_1)(i\mathfrak{D}_2)]. \tag{25}$$

The quantity $F_0^{(2)}$ of (15) and (16) equals the absorptive part in the case when the cut line goes between Reggeons; evidently there exist two possibilities:

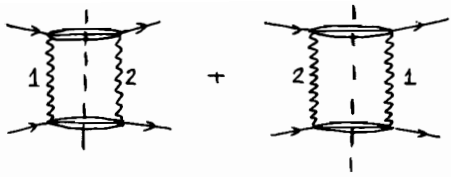

Correspondingly we get from (25)

$$F_0^{(2)} = \left[(i\mathfrak{D}_1)\,(i\mathfrak{D}_2)^*\right] + \left[(i\mathfrak{D}_2)\,(i\mathfrak{D}_1)^*\right] = 2\left[\mathrm{Re}\mathfrak{D}_1\,\mathrm{Re}\mathfrak{D}_2 + \mathrm{Im}\mathfrak{D}_1\,\mathrm{Im}\mathfrak{D}_2\right]. \tag{26}$$

The absorptive parts $F_1^{(2)}$ correspond to "cutting" of one of the Reggeons; we have four possibilities

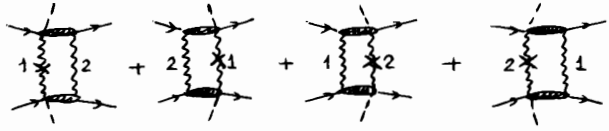

We get from (25)

$$\begin{aligned} F_1^{(2)} &= \left[(-i\delta\mathfrak{D}_1)\,(i\mathfrak{D}_2)^*\right] + \left[(i\mathfrak{D}_2)\,(-i\delta\mathfrak{D}_1)\right] + \left[(i\mathfrak{D}_1)\,(-i\delta\mathfrak{D}_2)\right] + \left[(-i\delta\mathfrak{D}_2)\,(i\mathfrak{D}_1)^*\right] \\ &= -8\left[\mathrm{Im}\mathfrak{D}_1\,\mathrm{Im}\mathfrak{D}_2\right], \end{aligned} \tag{27}$$

where $\delta\mathfrak{D} = 2i\,\mathrm{Im}\mathfrak{D}$ is a discontinuity of the amplitude $\mathfrak{D}$ over the right hand cut. At a simultaneous cutting of two Reggeons we have only one possibility

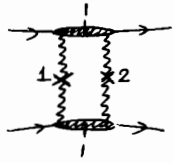

We find from (25)

$$F_2^{(2)} = \left[(-i\delta\mathfrak{D}_1)\,(-i\delta\mathfrak{D}_2)\right] = 4\left[\mathrm{Im}\mathfrak{D}_1 \cdot \mathrm{Im}\mathfrak{D}_2\right]. \tag{28}$$

Adding (26), (27), and (28) we have

$$F_0^{(2)} + F_1^{(2)} + F_2^{(2)} = 2\left[\mathrm{Re}\mathfrak{D}_1 \cdot \mathrm{Re}\mathfrak{D}_2 - \mathrm{Im}\mathfrak{D}_1 \cdot \mathrm{Im}\mathfrak{D}_2\right]. \tag{29}$$

This evidently coincides with the value for $2\,\mathrm{Im}A^{(2)}$, which is found directly from (25). Relation (29) shows that the sum $F_0^{(2)} + F_1^{(2)} + F_2^{(2)}$ really "saturates" the quantity $2\,\mathrm{Im}A^{(2)}$. Such a result is not trivially evident, since Feynman diagrams show (see the previous section) that $A^{(2)}$ could also have other types of absorptive parts. Our argument that these other absorptive parts are asymptotically small was based on the fact that for these large q_i^2 would be on virtual lines. But,

in fact, just such suppression of large q_i^2 leads to a factorized structure of the integrand in (23), for which relation (16) holds exactly.

In a similar way the absorptive parts $F_\mu^{(\nu)}$ are obtained corresponding to cutting of μ Reggeons in contribution (23). First we consider the case when $\mu \neq 0$. Then due to cutting of μ Reggeons a factor

$$\prod_{\beta=1}^{\mu}(-i\delta\mathcal{D}_\beta) = \prod_{\beta=1}^{\mu}(2\,\mathrm{Im}\mathcal{D}_\beta)$$

appears from (23) and each uncut Reggeon may be situated both to the right and to the left of the line of cutting; this gives a factor

$$\prod_{\gamma=\mu+1}^{\nu}\left[(i\mathcal{D}_\gamma)+(i\mathcal{D}_\gamma)^*\right] = \prod_{\gamma=\mu+1}^{\nu}(-2\,\mathrm{Im}\mathcal{D}_\gamma).$$

Hence

$$F_\mu^{(\nu)} = \sum_{\{\mu\}}\prod_{\beta=1}^{\nu}(-1)^{\nu-\mu}(2\,\mathrm{Im}\mathcal{D}_\beta), \tag{30}$$

where summation is made over all possible sets of cut Reggeons. Since

$$\mathrm{Im}\mathcal{D}_\beta = \pm e^{\xi\left[\alpha_\beta(0)-1-\alpha'\kappa_\beta^2\right]},$$

all the terms in (30) are the same. Since μ Reggeons may be extracted from ν Reggeons in $C_\nu^\mu = \nu!/\mu!(\nu-\mu)!$ ways, we finally get ($\mu \neq 0$):

$$F_\mu^{(\nu)} = (-1)^{\nu-\mu}C_\nu^\mu\prod_{\beta=1}^{\nu}(2\,\mathrm{Im}\mathcal{D}_\beta). \tag{31}$$

The expression for $F_0^{(\nu)}$ may be written in the form

$$F_0^{(\nu)} = \prod_{\beta=1}^{\nu}\left[(i\mathcal{D}_\beta)+(i\mathcal{D}_\beta)^*\right] - \prod_{\beta=1}^{\nu}(i\mathcal{D}_\beta) - \prod_{\beta=1}^{\nu}(i\mathcal{D}_\beta)^*,$$

where the last two terms take into account the fact that all Reggeons cannot be at one side of the cut line. Finally we have

$$F_0^{(\nu)} = (-1)^\nu\prod_{\beta=1}^{\nu}(2\,\mathrm{Im}\mathcal{D}_\beta) + 2\,\mathrm{Im}\left[-i\prod_{\beta=1}^{\nu}(i\mathcal{D}_\beta)\right]. \tag{32}$$

As before, we get from (31) and (32)

$$\sum_{\mu=0}^{\nu}F_\mu^{(\nu)} = 2\,\mathrm{Im}\left[(-i)\prod_{\beta=1}^{\nu}(i\mathcal{D}_\beta)\right], \tag{33}$$

which coincides with $2\,\mathrm{Im}\,A^{(\nu)}$ from (23). Note that the relations

$$\sum_{\mu=1}^{\nu} \mu F_{\mu}^{(\nu)}(s,t) = \left[(-1)^{\nu}\prod_{\beta=1}^{\nu}(2\,\mathrm{Im}\mathfrak{D}_{\beta})\right]\sum_{\mu=1}^{\nu}(-1)^{\mu}\mu C_{\nu}^{\mu} = 0, \tag{34}$$

. . . . . ,

$$\sum_{\mu=m}^{\nu} \mu(\mu-1)\ldots(\mu-m+1)F_{\mu}^{(\nu)}(s,t) = 0 \tag{34'}$$

follow from (31); they are found to be very important in calculations of corrections for inclusive cross sections.

Generalization to arbitrary Regge diagrams is self evident. The contribution of each diagram may be written as an integral of the type (23) of the product of $\mathfrak{D}_i$ and vertex functions. Here the integration is performed over the values of energy variables of different Reggeons. Evidently it is always possible to isolate the "complex" part of the integrand in the form (23'). Further, absorptive parts are found in a way similar to that used in the absence of interaction of Reggeons. But there is one important distinction. The cut line passes through a number of vertices of interactions between Reggeons and we must know what happens to these vertices at their "cutting".

The vertices N_{ν} are not changed by cutting for any diagrams in the perturbation theory. That means firstly the exact vertices N_{ν}, in which interactions between Reggeons are taken into account, also are not changed by cutting and secondly $\Gamma_{1\to\nu}$ vertices of the transition of one Reggeon into ν Reggeons are not changed by cutting

All the other vertices $\Gamma_{\nu_1\to\nu_2}$, $\nu_1,\ \nu_2 \geq 2$

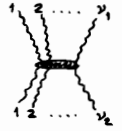

generally speaking are changed by cutting. This can be seen both from the consideration of Feynman diagrams for $\Gamma_{\nu_1\to\nu_2}$ and also from the following observations. Let us take the simplest diagrams for $\Gamma_{2\to 2}$ in the Reggeon perturbation theory (the constant r is small).

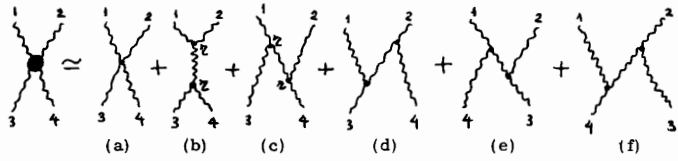

(35)

We see that if all Reggeons are cut [or at least (1-2) or (3-4)] then all the diagrams (a) - (f) contribute to the cut $\Gamma_{2\to 2}$. But, if the cut, for instance, passes between Reggeons, then only the diagrams (a) and (b) contribute; the contributions of the other ones will be asymptotically small. Hence, the ratio between values of cut vertices will depend on the value of r.

Thus, in the general case, to calculate absorptive parts of arbitrary Reggeon diagrams, it is also necessary to know the values of the cut vertices.

3. Inclusive Cross Sections

It is convenient to describe inclusive processes $p_a + p_b \to p + \{X\}$, $p_a + p_b \to p_1 + p_2 + \{X\}$, etc. by means of invariant inclusive cross sections

$$f_1(p) = (2\pi)^3 2p_0\left(\frac{\partial^3\sigma}{\partial p^3}\right)$$

$$f_2(p_1, p_2) = (2\pi)^6 4p_{10}p_{20}\left(\frac{\partial^6\sigma}{\partial p_1^3 \partial p_2^3}\right), \text{ etc.}$$

For any particle of momentum p we choose as kinematic variables, $p_\perp^2$, $\eta_1 = \ln(p_a + p)^2$, $\eta_2 = \ln(p_b + p)^2$, where $\eta_1 + \eta_2 = \xi$, and limit ourselves to consideration of the central region, where $\eta_1, \eta_2 \to \infty$. Here the main, energy-independent contribution to f_1 appears from the diagram:[8,9]

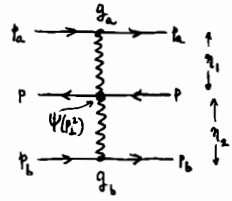

(36)

and has the form

$$f_1\left(p_\perp^2, \infty, \infty\right) = g_a(0)\psi\left(p_\perp^2\right) g_b(0). \tag{37}$$

The meaning of the quantities in (37) is clear from (36). Diagram (36) for f_1 is obtained from the Reggeon diagram for forward elastic scattering. The absorptive part is taken from it and a particle with the momentum p is "isolated" from the Reggeon; as a result a new vertex $\psi\left(p_\perp^2\right)$ appears in the diagram. A similar procedure leads to more complicated Reggeon diagrams for f_1. Namely, we take one of the asymptotically surviving absorptive parts of the diagram for $A_{2\to 2}$ and join the vertex $\psi\left(p_\perp^2\right)$ to one of the "cut" lines. Since in a given Reggeon diagram the other lines may be both cut and not cut, it is also necessary to sum up all contributions obtained in this way over all these possibilities. Thus we come to the Reggeon diagram (38) for f_1 in which μ of the ν Reggeon lines are cut. In fact, we consider the general case, since the vertices themselves can contain arbitrary Reggeon diagrams. To obtain the contribution of (38) to f_1, it is necessary to perform

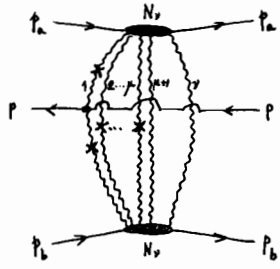

(38)

the following operation,

$$(\mathrm{abs})_s[-i(i\hat{D}_1)(i\hat{D}_2)\ldots(i\hat{D}_\nu)] \tag{39}$$

with the Green functions of Reggeons and in addition make the substitution

$$\mathrm{Im}\hat{D} \to (\mathrm{Im}\hat{D})\cdot\psi\left(p_\perp^2\right)(\mathrm{Im}\hat{D}). \tag{40}$$

Since such a substitution can be carried out for each cut line, an additional factor μ appears in the contribution. Then, taking into account (31) we obtain the expression for the contribution of (38) to f_1:

$$\begin{aligned}(f_1)^{\nu,\mu} = (-1)^{\nu-\mu}\cdot\mu\, C_\nu^\mu \int d\Omega_\nu \cdot N_\nu\left\{\left[2\,\mathrm{Im}\hat{D}_1\cdot\psi\left(p_\perp^2\right)\mathrm{Im}\hat{D}_1\right]\right\}\cdot \\ \cdot(2\,\mathrm{Im}\hat{D}_2)(2\,\mathrm{Im}\hat{D}_3)\ldots\left[(2\,\mathrm{Im}\hat{D}_2)\right]N_\nu.\end{aligned} \tag{41}$$

Here it is assumed that the vertex N_ν is not changed by cutting. Hence, we obtain the relation

$$\sum_{\mu=1}^{\nu}(f_1)^{\nu,\mu} = 0 \qquad ,\ \nu \geq 2, \tag{42}$$

similar to (34), from which it follows that diagram (38) in general do not contribute to f_1. Only the contribution of diagram (36) with the exact Green functions and vertices* is left (it will be considered in the next section). If we imagine that Reggeons do not interact one with the other, then f_1 is given by relation (37) and corrections to f_1 that vanish as powers of $1/\eta_i$ are absent. The first nonvanishing corrections for (37) are obtained by taking into account nonvacuum trajectories in diagram (36); at the same time there are logarithmic corrections in total cross sections due to diagram (17). But, in fact, the interaction between Reggeons is not zero. This leads to additional

*We remark here that due to (42) eikonal models[10] with "input" trajectory $\alpha(0)>1$ appear to be inconsistent. Because of the described compensation only the pole term was left in f_1, i.e., $f_1(p_\perp^2, \eta, \xi) \sim \psi(p_\perp^2)s^{\alpha(0)-1}$ in the central region. Furthermore, in the sum rule related to energy conservation

$$\sigma_{\mathrm{tot}}^{-1}\int d^2p_\perp \int_{\eta_1}^{\eta_2} d\eta\, e^{\eta-\xi} f_1\left(p_\perp^2, \eta, \xi\right) \leq 1,$$

we choose the upper limit $\eta_2 = C\xi$ in such a way that $1 > C > 2 - \alpha(0)$. Then on the one hand, we do not leave the central region and on the other we come to a violation of the sum rule if $\alpha(0) - 1 > 0$.

[beyond (36) and (38)] contributions to f_1, which correspond to the situation when the "observed" particle is "emitted" from the vertex of interaction of Reggeons. Such a mechanism of particle production gives, for instance, from the diagram for $A_{2\to 2}$ the following diagrams for f_1:

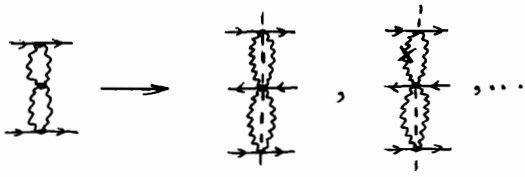

The contributions of these diagrams to f_1 are small ($\sim 1/\eta_1^2\eta_2$, $1/\eta_1\eta_2^2$).

Let us consider now what diagrams will be important for double inclusive cross sections $f_2(p_1, p_2)$. The arguments of f_2 are $\eta_1 = \ln(p_a+p_1)^2$, $\eta_2 = \ln(p_1+p_2)^2$, $\eta_3 = \ln(p_2+p_b)^2$, $\eta_1+\eta_2+\eta_3 \simeq \xi$, $p_{1\perp}$ and $p_{2\perp}$. When all η_i are large, the main contribution to f_2 appear from the diagrams

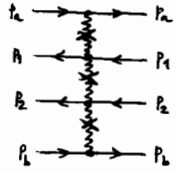

(43)

and has the form:

$$f_2(p_{1\perp}, p_{2\perp}, \infty, \infty, \infty) = g_a\psi\left(p_{1\perp}^2\right)\psi\left(p_{2\perp}^2\right)g_b = \sigma_{tot}^{-1} f_1(p_1) f_1(p_2). \tag{44}$$

Let us find now what diagrams will lead to corrections for (44). Let us consider the diagrams for f_2, similar to (38)

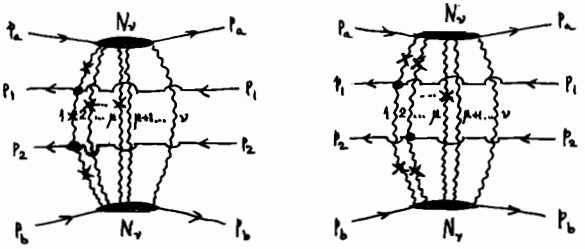

where, just as in (38), it is necessary to sum over the number of cut Reggeons. Using relations (34) and (34') it is easy to see that the contributions of all these diagrams (with exact N_ν) are cancelled like (42), except for the two Pomeron contribution.

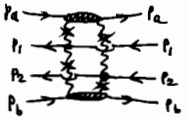

(45)

There are also diagrams for f_2 where Reggeons interact "between" particles "1" and "2"

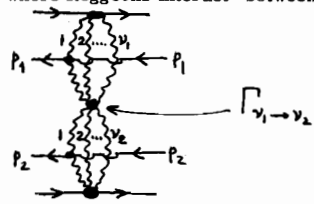

(46)

Since the vertices $\Gamma_{\nu_1 \to \nu_2}$ for ν_1, $\nu_2 \geq 2$ are generally changed by cutting the diagrams (46) all contribute to f_2, except for the cancelled diagrams

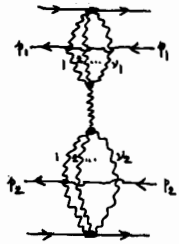

Similarly to the case of f_1, small contributions are also left when the "observed" particles "1" and "2" are produced at the point of interaction of Reggeons:

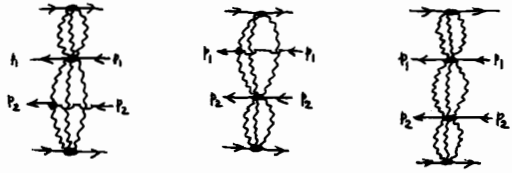

4. Main Corrections to Inclusive Cross Sections in the Central Region

As was shown in the previous section, the dominant contribution to f_1 as η_1, $\eta_2 \to \infty$ and the main corrections to it are determined by diagram (36) with exact vertices g and exact vacuum Green functions $\mathfrak{D}$. Having the aim to find the main corrections for f_1 (∞) of the order $1/\eta_1$, we can limit ourselves to terms linear in g and quadratic in $\mathfrak{D}$ in the triple-Pomeron vertex r (we recall that $r = 0$ when $k_{i\perp} = 0$[10]). Hence it suffices to find the total contribution to f_1 from the diagrams

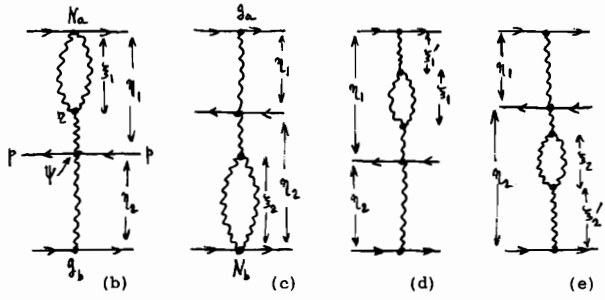

(47)

The contributions of the diagrams (b - e) to f_1 have the form

$$f^{(b)} = \left[\int_1^{\eta_1} d\xi_1 \sum_a' (\xi_1) \right] \psi g_b,$$

$$f^{(c)} = g_a \psi \left[\int_1^{\eta_2} d\xi_2 \sum_b' (\xi_2) \right],$$

$$f^{(d)} = g_a \left[\int_1^{\eta_1} d\xi_1 \sum (\xi_1) \int_1^{\eta_1 - \xi_1} d\xi_1' \right] \psi g_b, \tag{48}$$

$$f^{(e)} = g_a \psi \left[\int_1^{\eta_2} d\xi_2 \sum (\xi_2) \int_1^{\eta_2 - \xi_2} d\xi_2' \right] g_b,$$

where $\sum_i' (\xi)$ and $\sum (\xi)$ are contributions of Reggeon loops:

$$\sum_i' (\xi) = -\int \frac{d^2 k_\perp}{4(2\pi)^2} N_i\left(k_\perp^2\right) e^{-2\alpha' k_\perp^2 \xi} r\left(k_\perp^2\right),$$

$$\sum (\xi) = -\int \frac{d^2 k_\perp}{4(2\pi)^2} r\left(k_\perp^2\right) e^{-2\alpha' k_\perp^2 \xi} r\left(k_\perp^2\right). \tag{49}$$

At small $k_\perp^2$

$$r\left(k_\perp^2\right) \simeq 2\beta\alpha' k_\perp^2, \quad N_i\left(k_\perp^2\right) \simeq N_i.$$

Therefore at large ξ we get from (49)

$$\sum_i' (\xi) \simeq -\frac{1}{\xi^2} \frac{N_i \beta}{32\pi\alpha'}, \quad \sum (\xi) = -\frac{1}{\xi^3} \frac{\beta^2}{16\pi\alpha'}. \tag{49'}$$

Further, the expressions (48) for $f^{(b)}$—$f^{(e)}$ must be renormalized, corresponding to subtraction of polynomial parts in η_i from them. Such renormalization is unambigous. Adding the subtracted terms to the contribution of the pole diagram, we get the renormalized pole term,

$$\tilde{f}^{(a)} = g_a \psi g_b.$$

Renormalization of the integrals in (48) is best carried out by means of the identities

$$\int_1^{\eta_1} d\xi_1 \sum_1' (\xi_1) = \int_1^{\infty} d\xi_1 \sum' (\xi_1) - \int_{\eta_1}^{\infty} d\xi_1 \sum' (\xi_1),$$

$$\int_1^{\eta_1} d\xi_1 \sum (\xi_1) \int_1^{\eta_1 - \xi_1} d\xi_1' = \int_1^{\infty} (\eta_1 - \xi_1) \sum (\xi_1) d\xi_1 + \int_{\eta_1}^{\infty} d\xi_1 (\xi_1 - \eta_1) \sum (\xi_1). \tag{50}$$

Taking into account the behavior of $\sum'(\xi)$ and $\sum(\xi)$ at $\xi \to \infty$ we note that the last integrals in (50) already do not contain polynomial parts. Thus the renormalized expressions for $\tilde{f}^{(i)}$ will take the form,

$$\tilde{f}^{(a)} = g_a \psi g_b,$$

$$\tilde{f}^{(b)} = -\left[\int_{\eta_1}^{\infty} d\xi_1 \sum_a'(\xi_1)\right] \psi g_b \simeq N_a \left(\frac{\beta}{32\pi\alpha'\eta_1}\right) \psi g_b,$$

$$\tilde{f}^{(c)} = -g_a \psi \left[\int_{\eta_2}^{\infty} d\xi_2 \sum_b'(\xi_2)\right] \simeq g_a \psi \left(\frac{\beta}{32\pi\alpha'\eta_2}\right) N_b, \tag{51}$$

$$\tilde{f}^{(d)} = g_a \left[\int_{\eta_1}^{\infty} d\xi_1 (\xi_1 - \eta_1) \sum(\xi_1)\right] \psi g_b \simeq g_a \left(-\frac{\beta^2}{32\pi\alpha'\eta_1}\right) \psi g_b,$$

$$\tilde{f}^{(e)} = g_a \psi \left[\int_{\eta_2}^{\infty} d\xi_2 (\xi_2 - \eta_2) \sum(\xi_2)\right] g_b \simeq g_a \psi \left(-\frac{\beta^2}{32\pi\alpha'\eta_2}\right) g_b.$$

Adding these contributions we get

$$f_1 = g_a \psi\left(p_\perp^2\right) g_b \left(1 + \frac{c_a}{\eta_1} + \frac{c_b}{\eta_2}\right), \tag{52}$$

$$c_i = \frac{\beta}{32\pi\alpha' g_i} (N_i - g_i \beta). \tag{53}$$

With the same degree of accuracy as before, i.e., omitting all terms of higher order in $1/\eta_i$, expressions (53) may still be simplified. This follows from the fact that in the regime of constant total cross sections a number of additional conditions should be used for the vertices of interaction of vacuum Reggeons. Firstly, at vanishing Pomeron momentum all vertices of diffraction association must vanish. Therefore N_i takes the eikonal form, $N_i = g_i^2$, and

$$c_i = \frac{\beta}{32\pi\alpha'} (g_i - \beta).$$

Further it was shown[6] that under the same assumptions all $g_i(0)$ are equal: $g_i^2(0) = \sigma_{tot}(\infty)$, independent of the types of colliding hadrons. In this case, all the c_i are the same

$$c_i = c = \frac{\beta}{32\pi\alpha'} \left(\sqrt{\sigma_{tot}(\infty)} - \beta\right), \tag{54}$$

and f_1 takes a form symmetric in η_i:

$$f_1(p_\perp, \eta_1, \eta_2) = \sigma_{tot} \psi\left(p_\perp^2\right) \left[1 + c\left(\frac{1}{\eta_1} + \frac{1}{\eta_2}\right)\right]. \tag{55}$$

Evidently, f_1 will have a maximum at $\eta_1 = \eta_2 = \xi/2$ if $c < 0$ and a minimum if $c > 0$. In the variables $\xi = \eta_1 + \eta_2$, $y = (\eta_1 - \eta_2)/2$, we have

$$f_1(p_\perp, y, \xi) = \sigma_{tot}\psi\left(p_\perp^2\right)\left(1 + \frac{4c\xi}{\xi^2 - 4y^2}\right). \tag{56}$$

Let us only note that the sign of c cannot be determined from theoretical considerations at present.

It is interesting to compare the main asymptotic corrections for f_1 with the corrections of the order $1/\xi$ for σ_{tot}, which are determined by the diagrams:

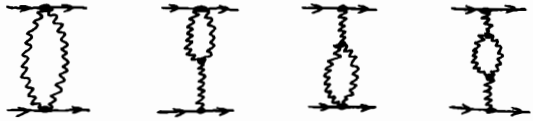

Renormalizing their contributions similarly to (51), we get:

$$\sigma_{tot}(\xi) \simeq \sigma_{tot}^{(\infty)}\left[1 - \frac{1}{32\pi\alpha' g_a g_b}\frac{1}{\xi}(N_a - g_a\beta)(N_b - g_b\beta)\right] \to$$

$$\to \sigma_{tot}^{(\infty)}\left[1 - \frac{(g-\beta)^2}{32\pi\alpha'\xi}\right] \equiv \sigma_{tot}^{(\infty)}\left(1 - \frac{32\pi\alpha' c^2}{\beta^2\xi}\right). \tag{57}$$

Let us consider now the main corrections for the double inclusive cross section f_2 and confine ourselves to the region $\eta_1, \eta_3 >> \eta_2 >> 1$., i.e., we look for the main corrections in $1/\eta_2$. It is easy to see that contributions to $f_2 \sim 1/\eta_2$ may appear only from the diagrams

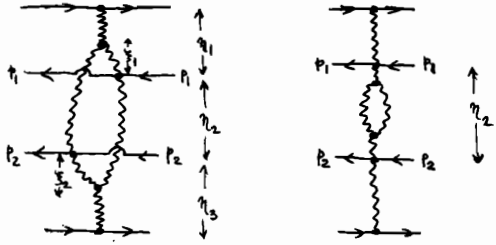

(58)

The contribution of diagram (a) at large η_2 is easily calculated and has the form

$$f_2^{(a)} = g_a\psi\left(p_{1\perp}^2\right)\left[\frac{\beta^2}{4\pi\alpha'}\int_1^{\eta_1} d\xi_1 \int_1^{\eta_3} \frac{d\xi_2}{(\eta_2 + \xi_1 + \xi_2)^3}\right]\psi\left(p_{2\perp}^2\right)g_b =$$

$$= g_a\psi\left(p_{1\perp}^2\right)\left(\frac{\beta^2}{8\pi\alpha'\eta_2}\right)\psi\left(p_{2\perp}^2\right)g_b. \tag{59}$$

The contribution of diagram (b) is determined by similar integrals, with the result,

$$f_2^{(b)} = -\frac{1}{4}f_2^{(a)}.$$

Then from (44) and (59) we get the expression for the two-particle correlation function,

$$\rho_2 \equiv \frac{f_2(p_1, p_2)}{\sigma_{tot}} - \frac{f_1(p_1)}{\sigma_{tot}} \frac{f_1(p_2)}{\sigma_{tot}} = \frac{1}{\eta_2} \frac{3\beta^2}{32\pi\alpha'} \psi\left(p_{1\perp}^2\right) \psi\left(p_{2\perp}^2\right). \tag{60}$$

It is interesting to note that the sign of ρ_2 at $\eta_2 >> 1$ is quite definite (positive).

5. Fluctuations of Distribution of Density of Produced Particles

At $\xi \to \infty$ the average number of particles produced in an interaction is great ($\bar{n} \simeq a\xi$). Hence the final state of an individual event may be described by means of the density of the produced particles $\nu(\eta)$ in rapidity space. Then the total number of particles,

$$n(\xi) = \int_1^\xi d\eta\, \nu(\eta), \tag{61}$$

will fluctuate from event to event. As was discussed in the introduction, "switching" of the Pomeron cuts leads to a very nontrivial structure [of the form (7)] for the distribution of the quantity $\eta(\xi)$. We now try to determine how often different types of functions $\nu(\eta)$ are encountered* and what physical mechanism is responsible for such fluctuations.

Averaged over many events, the quantity $\nu(\eta)$ is expressed by means of the inclusive cross section,

$$\overline{\nu(\eta)} = \sigma_{tot}^{-1} \int d^2p_\perp\, f_1(p_\perp, \eta, \xi). \tag{62}$$

Each cut Pomeron "ξ_i long" contains on the average a ξ_i particles. Therefore the mean distance between particles is $\sim a^{-1}$. Evidently the density $\nu(\eta)$ has meaning only after averaging over a distance long in comparison with a^{-1}; such an averaging will be understood in what follows.

There are two mechanisms leading to a deviation of the function $\nu(\eta)$ from the asymptotic mean value $\overline{\nu(\eta)} = a$. The first is the near correlation in a Pomeron, leading to fluctuations with a period of the order of some units of a^{-1}. Such a correlation is related to nonvacuum Reggeons.** As was already noted, we shall assume that an averaging is made over such fluctuations. The second mechanism is related to Pomeron branch points; it leads to long-range fluctuations of $\nu(\eta)$ with the periods up to ξ. These fluctuations will now be considered.

What type of functions $\nu(\eta)$ can be "encountered"? In section 1 we saw that all inelastic processes related to the absorptive parts of Reggeon diagrams may be divided into topologically nonequivalent classes. It is seen at once that a certain function $\nu(\eta)$ corresponds to each of these classes.

---

*Correctly defined probabilities of encountering different $\nu(\eta)$ are given by the variations of some functional $W[\nu(\eta)]$, which in its turn may be expressed in terms of all higher inclusive cross sections. However, here we shall not dwell upon this problem and will make only the "qualitative" considerations given in the text of the paper.

**These fluctuations of $\nu(\eta)$ related to nonvacuum Reggeons are of Poisson character (see, for instance[12]) and decrease exponentially with an increase of η.

All these functions are of a step type and take integer values at each point (if we measure η in the units of a^{-1}, the integers being equal to the number of cut Reggeons "at a given η."* For instance,

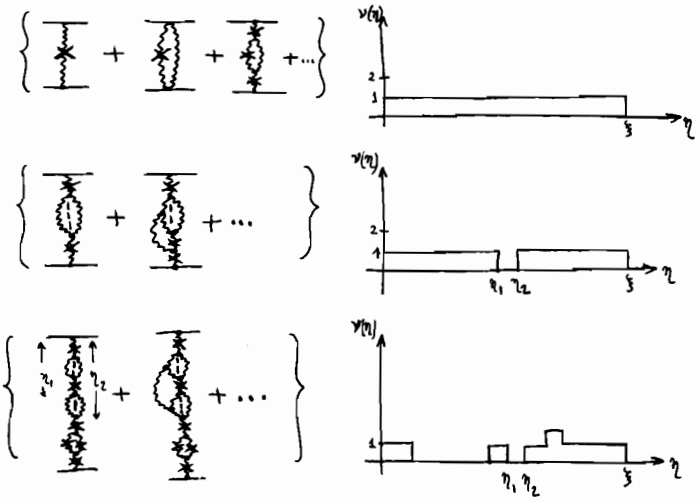

The functions $\nu(\eta)$ shown above correspond to the absorptive parts of Reggeon diagrams with bare Pomerons. Actually, only by cutting a bare Pomeron (with a finite radius of correlation in the ladder) do we get contributions to $\nu(\eta)$ independent of η in the range $\xi_1 < \eta < \xi_2$, where $\xi_2 - \xi_1$ is the energy invariant of the cut Pomeron.

However, we must have $\alpha(0) < 1$ [11] for a bare Pomeron.** Therefore the probability of finding a homogeneous configuration (63) disappears as a power in s. This also applies to any configuration with a fixed position of all steps. Therefore the most important problem is the finding the mean number of different inhomogeneities in the function $\nu(\eta)$ corresponding to predominant events.

Let us explain the suggested method by taking the example of the simplest inhomogeneity of $\nu(\eta)$, i.e., a gap, as shown in (63'). It is convenient to introduce $\hat{f}_1(\lambda, \eta, \xi)$, the inclusive cross section for production of the gaps of length λ and rapidity $= \eta$. The contribution of the diagram (63') for the fixed η_1 and η_2 with bare trajectories gives the cross section for production of gaps with the boundaries η_1 and η_2 in the background of a uniform distribution. Let us also consider other diagrams with bare Pomerons, which correspond to the functions $\nu(\eta)$, which have a gap on

*The system we consider has the properties of a one-dimensional gas in the volume ξ. A number of properties of this "Feynman gas" were discussed in literature (see Refs. 4 and 5). The non-exponential drop with the distance η of the correlation function ρ_2 shows that the case of constant total cross sections corresponds to the "Feynman gas" being at the critical point. From this point of view, the step function $\nu(\eta)$ corresponds to the fact that at the critical point the system is divided by fluctuations into regions which are in different "phase" states. It means that there are "phases" with different densities $\nu = 0, 1, 2, \ldots$ for the "Feynman gas". And if the Pomeron's $\alpha(0) < 1$ then the long-range fluctuations of $\nu(\eta)$ are damped as $|\eta_1 - \eta_2|^{-1} \exp\{-[1-\alpha(0)]|\eta_1 - \eta_2|\}$.

**Here, "bare" means homogeneous distributions in η, with all screening taking into account.

the interval (η_1, η_2) while outside this region they take arbitrary values. [An example of such diagrams is given in (63'')]. It is natural to identify the total contribution of all such diagrams with bare Pomerons at fixed η_1, η_2 with $\hat{f}_1(\lambda_1, \eta_1, \xi)$. But, on the other hand, the sum of these diagrams may be reexpressed as the sum of Reggeon diagrams with the exact, renormalized vertices and Green functions of Pomerons, for which $\alpha(0) = 1$. Then we shall have

$\hat{f}_1(\lambda, \eta, \xi) =$ 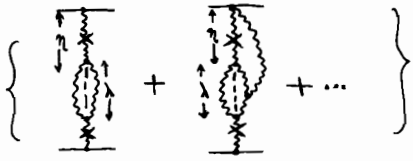 (64)

For $\lambda >> 1$ only the first diagrams predominate in this series. Hence

$$\hat{f}_1(\lambda, \eta, \xi) \simeq g\left[-\sum(\lambda)\right] g \simeq g^2 \frac{\beta^3}{16\pi\alpha'\lambda^3}, \tag{65}$$

where we have used expression (49') for $\sum(\lambda)$, and an extra (-1) appears due to cutting of $\sum(\lambda)$ "between" Reggeons. Diagrams (64) for $\hat{f}_1$ may be naturally compared to the diagram (36) for f_1. We see that (abs) $\sum(\lambda)$ plays the role of the vertex ψ in the diagram (36). Because of such a similarity in the structures for the diagrams for $\hat{f}_1$ and f_1, the conclusions of the previous sections concerning f_1 are naturally transferred to $\hat{f}_1$.

Further, the function $\hat{f}_1$ which is an inclusive cross section must satisfy the normalizing relation

$$\int f_1(\lambda, \eta, \xi) d\eta = \sigma_{tot} \langle m(\lambda) \rangle, \tag{66}$$

where $\langle m(\lambda) \rangle d\lambda$ is the mean multiplicity of gaps in $\nu(\eta)$ with the dimensions $(\lambda, \lambda + d\lambda)$. Substituting (65) into (66) we find

$$\langle m(\lambda) \rangle = \xi \left[(\text{abs}) \sum(\lambda)\right] = \xi \frac{\beta^2}{16\pi\alpha'\lambda^3}. \tag{67}$$

This relation is interesting firstly because it gives an explicit form of $\langle m(\lambda) \rangle$ at large λ and secondly it gives a new s-channel meaning for the self-energy part $\sum(\lambda)$.

Evidently, the above considerations are at once transferred to other forms of inhomogeneities of the function $\nu(\eta)$. Diagrams (64), but with both cut Reggeons in $\sum(\lambda)$

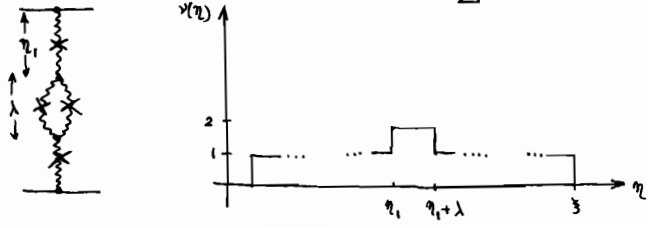

(68)

also give an inclusive cross section for mesa* production [$\nu(\eta) = 2$ in the range η_1, $\eta_1 + \lambda$]. Using (26) and (28) we get immediately

$$<m(\lambda)>_{\text{mesa}} = 2<m(\lambda)>_{\text{gap}}. \tag{69}$$

Similarly, the absorptive parts of more complex diagrams for $\sum(\lambda)$ give the inclusive cross sections for production of the analogous inhomogeneities of $\nu(\eta)$.

Evidently, for large λ, inhomogeneities of the gap type and of the mesas with $\nu = 2$ predominate, since $\hat{f}_1$ for more complex fluctuations contains a higher power of λ in the denominator.** Hence below we limit ourselves to consideration of those simplest inhomogeneities of $\nu(\eta)$. The quantity

$$\overline{m(\lambda)} = \int_{\lambda}^{\infty} d\lambda' <m(\lambda')> \tag{70}$$

gives the mean multiplicity of gaps (mesas) with dimensions larger than λ. We have from (67)

$$\overline{m(\lambda)} \simeq \xi \frac{\beta^2}{32\pi\alpha'\lambda^2} \tag{71}$$

Hence we find that the mean distance between neighboring gaps with dimensions $\sim\lambda$ will be of the order,

$$\frac{32\pi\alpha'}{\beta^2}\lambda^2 >> \lambda \text{ at } \lambda >> 1. \tag{72}$$

Thus we see that gaps form a "rarified gas" for which the mean value of the correlation function is $\hat{\rho}_2 \sim 1/\lambda^2 << 1$. It therefore follows that the probabilities w_m to find m gaps or mesas with dimensions larger than $\lambda >> 1$ in the system are distributed according to the Poisson law with the mean number $\overline{m(\lambda)}$:

$$w_m = \frac{e^{-\overline{m(\lambda)}}}{m!}[\overline{m(\lambda)}]^m. \tag{73}$$

For $\lambda \sim \lambda_{max} = \beta\sqrt{\xi/32\pi\alpha'}$ the quantity $\overline{m(\lambda_{max})} \sim 1$. This means that the gap (mesa) spectrum is concentrated in the region

$$\lambda_{max} \geq \lambda \geq \lambda_0 \sim 1. \tag{74}$$

When $\lambda >> \lambda_{max}$ the quantity $\overline{m(\lambda)} << 1$ has the meaning of the probability of finding one gap (mesa) with dimension $\geq\lambda$ in an individual event.

Our considerations show that $\nu(\eta)$, on the average, must have (with the weight ~ 1) the following structure: there is about one gap (and two mesas) with dimensions $\sim \lambda_{max} = \gamma\sqrt{\xi}$; of the order of four gaps (and doubled number of mesas) with dimensions $\sim\lambda_{max}/2$, etc. down to values of λ of the order of the correlation length.

*Mesa is Spanish for table or plateau. In the American southwest, geological formations called mesas, closely similar in shape to the rectangular enhancements in $\nu(\eta)$ shown above, are a familiar sight to the traveler. -Ed.

**We are not going to consider here the problem of the "fine structure" of the mesas. The dimensions of such inhomogeneities will be $\lesssim\sqrt{\lambda/32\pi\alpha'}$. In such a case, for "observation" of the inhomogeneities of $\nu(\eta)$ with dimensions $\geq\lambda$, it is necessary to average $\nu(\eta)$ over the intervals $\lesssim\beta\sqrt{\lambda/32\pi\alpha'}$.

Thus we see that the structure of the actual function $\nu(\eta)$ is very inhomogeneous* and will only weakly resemble $\nu(\eta) = \text{constant}$, characterizing a simple multiperipheral chain.

In conclusion we indicate what phenomena may be expected in individual many-particle events, at nonasymptotic ξ. When ξ is such that $\lambda_{max} = \gamma\sqrt{\xi} \lesssim \lambda_0$, where λ_0 is the correlation length related to nonvacuum Reggeons ($\lambda_0 \sim 1\text{-}2$), most of the events will be generated with homogeneous $\nu(\eta)$. But when $\gamma\sqrt{\xi}$ becomes greater than λ_0, a gap or a mesa with dimensions larger than the correlation length will be encountered in individual events (with the weight = 1). With further increase of ξ a second inhomogeneity may appear, etc.

The described behavior of $\nu(\eta)$ resembles that discussed for many years (mainly in the literature devoted to cosmic ray physics): observation of considerable inhomogeneities in individual many-particle events whose explanation was given (in the same literature) in terms of a fire-ball hypothesis. However, our considerations show that large inhomogeneities of $\nu(\eta)$ perhaps may be also explained without new physical ideas.

Finally, we should like to thank L. N. Lipatov and K. A. Ter-Martirosyan for interesting discussions.

References

[1] D. Amati, A. Stanghellini, and S. Fubini, Nuovo Cimento 26, 896 (1962).

[2] V. N. Gribov, Zh. Exp. Teor. Fiz. 53, 654 (1967) [Sov. Phys. JETP 26, 414 (1968)].

[3] V. A. Abramovskii, O. V. Kancheli, Pis'ma v Zh. Exp. Teor. Fiz. 15, 559 (1972), [JETP Lett. 15, 397 (1972)].

[4] K. Wilson, Cornell preprint CLNS-131 (November, 1970).

[5] J. D. Bjorken, Particles and Fields - 1971, AIP Conf. Proc. No. 2, Particles and Fields Subseries No. 1, DPF Divisional Meeting, Rochester, N.Y., Aug. 30-Sept. 2, 1971, ed. A. C. Melissinos and P. F. Slattery, Am. Inst. Phys., N.Y. (1972), p. 110.

[6] V. N. Gribov, these Proceedings.

[7] S. Mandelstam, Nuovo Cimento 30, 1127, 1148 (1963).

[8] A. Mueller, Phys. Rev. D2, 2963 (1970).

[9] V. A. Abramovskii, O. V. Kancheli, I. D. Mandzhavidze, Yad. Fiz. 13, 1102 (1971), [Sov. J. Nucl. Phys. 13, 630 (1971)].

[10] H. Cheng, T. T. Wu, Phys. Rev. Letters 24, 1456 (1970).

[11] V. N. Gribov, A. A. Migdal, Yad. Fiz. 8, 1002 (1968) [Sov. J. Nucl. Phys. 8, 583 (1969)].

[12] A. Mueller, Phys. Rev. D4, 150 (1971).

Appendix

We give here simple arguments showing that N_ν is not changed by different cuttings. The vertex N_ν appears in calculation of the asymptotics of Feynman diagrams

*Some conclusions of this section are similar to results available in the paper of K. A. Ter-Martirosyan presented at the conference, paper #932.

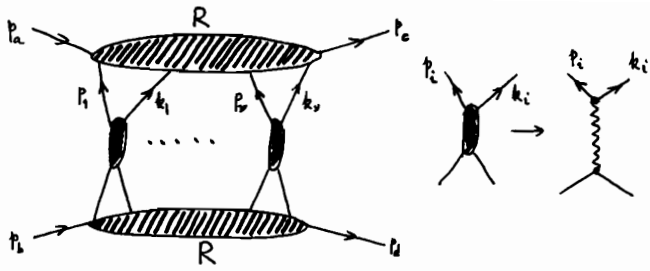

(A1)

and may be written in the form[2]

$$N_\nu = \int_{-\infty}^{+\infty} \prod_1^\nu \frac{d(\alpha_i s) d(\tilde{\alpha}_i s)}{Z_i \cdot \tilde{Z}_i} \delta\left[\sum_1^\nu (\alpha_i + \tilde{\alpha}_i)\right] \left[\prod_1^\nu \frac{d\beta_i d^2 p_{i\perp}}{2} g_i \beta_i^{J_i}\right] R, \tag{A2}$$

where

$$p_i = \alpha_i p_b' + \beta_i p_a' + p_{i\perp}, \quad k_i = \tilde{\alpha}_i p_b' + \beta_i p_a' + k_{i\perp}, \quad (p_a')^2 = (p_b')^2 = 0,$$

$$Z_i = p_i^2 - m^2 + i\epsilon, \quad \tilde{Z}_i = k^2 - m^2 + i\epsilon,$$

J_i are complex momenta of Reggeons and R is the amplitude of the process

(A3)

In (A2), integration over α_i, $\tilde{\alpha}_i$ is carried out with the Feynman $i\epsilon$ rule, and over β with finite limits ($\beta_i > 0$). It is also important (see Ref. 11) that the factors $B_i^{J_i}$ do not lead to new singularities in α_i, $\tilde{\alpha}_i$.

The main observation for us is that the amplitude R is integrated over the α-variables of all lines (p_i, k_i) completely symmetrically, independent of whether given lines are connected to one Reggeon or to different ones.

Let us consider the absorptive parts of the diagram (A1) when μ of the ν Reggeons are cut, μ_1 are on the left-hand side of the line of cutting and the other μ_2 on the right hand.

Then the cut vertex N_ν takes the form

$$N_\nu^{(\mu, \mu_1, \mu_2)} = \int_0^\infty d\gamma \delta[\gamma - (\alpha + \alpha_L)] \int_{-\infty}^{+\infty} \prod_1^\nu \frac{d(\alpha_i s) d(\tilde{\alpha}_i s)}{Z_i \cdot \tilde{Z}_i} \cdot$$

$$\cdot \delta\left[\sum_1^\nu (\alpha_i + \tilde{\alpha}_i)\right] \left[\prod_1^\nu \frac{d\beta_i d^2 p_{i\perp}}{2} g_i \beta_i^{J_i}\right] \cdot \left[(\mathrm{abs})_W R\right], \tag{A4}$$

where $(abs)_W R$ is the absorptive part of R in the variable $W = \gamma s$ corresponding to the following regrouping of lines

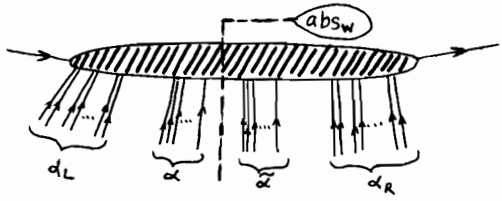

(A5)

But the vertex N_ν itself may be written in the same form (A4). Thus, we can always multiply the right-hand side of (A2) by

$$\int_{-\infty}^{+\infty} d\gamma \delta [\gamma - (\alpha + \alpha_L)]$$

and then deform the contour of integration over γ around the right-hand cut of the amplitude R. Then we come to expression (A4) for N_ν.